High Resolution Structural Analyses of Mutant Chitinase A Complexes with Substrates Provide New Insight into the Mechanism of Catalysis[†,‡]

Yannis Papanikolau,[§] Gali Prag,[||] Giorgos Tavlas,[§] Constantinos E. Vorgias,[⊥] Amos B. Oppenheim,[||] and Kyriacos Petratos*,[§]

Institute of Molecular Biology and Biotechnology, Foundation for Research and Technology-Hellas, P.O. Box 1527, 71110 Heraklion, Greece, Department of Molecular Genetics and Biotechnology, The Hebrew University, Hadassah Medical School, P.O. Box 12272, 91120 Jerusalem, Israel, and National and Kapodistrian University of Athens, Faculty of Biology, Department of Biochemistry Molecular Biology, 15784 Athens, Greece

ABSTRACT: Chitinase A (ChiA) from the bacterium *Serratia marcescens* is a hydrolytic enzyme, which cleaves β-1,4-glycosidic bonds of the natural biopolymer chitin to generate di-*N*-acetyl-chitobiose. The refined structure of ChiA at 1.55 Å shows that residue Asp313, which is located near the catalytic proton donor residue Glu315, is found in two alternative conformations of equal occupancy. In addition, the structures of the cocrystallized mutant proteins D313A, E315Q, Y390F, and D391A with octa- or hexa-*N*-acetyl-glucosamine have been refined at high resolution and the interactions with the substrate have been characterized. The obtained results clearly show that the active site is a semiclosed tunnel. Upon binding, the enzyme bends and rotates the substrate in the vicinity of the scissile bond. Furthermore, the enzyme imposes a critical "chair" to "boat" conformational change on the sugar residue bound to the −1 subsite. According to our results, we suggest that residues Asp313 and Tyr390 along with Glu315 play a central role in the catalysis. We propose that after the protonation of the substrate glycosidic bond, Asp313 that interacts with Asp311 flips to its alternative position where it interacts with Glu315 thus forcing the substrate acetamido group of −1 sugar to rotate around the C2−N2 bond. As a result of these structural changes, the water molecule that is hydrogen-bonded to Tyr390 and the NH of the acetamido group is displaced to a position that allows the completion of hydrolysis. The presented results suggest a mechanism for ChiA that modifies the earlier proposed "substrate assisted" catalysis.

Chitinases (EC 3.2.1.14) are widespread in nature. They are found in bacteria, fungi, plants, invertebrates, and all classes of vertebrates including human. These enzymes hydrolyze the abundant natural biopolymer chitin, producing smaller chito-oligosaccharides (*1*). Chitin consists of multiple *N*-acetyl-D-glucosamine (NAG)[1] residues connected via β-1,4-glycosidic linkages and is an important structural element of fungal cell wall and arthropod exoskeletons. On the basis of the mode of chitin hydrolysis, chitinases are classified as random, endo-, and exo-chitinases (*2*) and based on sequence criteria, chitinases belong to families 18 and 19 of glycosyl hydrolases (*3*). Mammalian chitinases were only recently discovered. The first human chitinase with a chitotriosidase activity was found to be specifically expressed by phagocytes (*4*). A similar lung specific chitotriosidase was also identified (*5*). More recently, an acidic mammalian chitinase (AMCase) was identified. This protein appears to be abundant in the gastrointestinal tract (*6*). These proteins may contribute to the defense against invading pathogens.

Chitinase A (ChiA) from *Serratia marcescens* belongs to glycosyl hydrolase family 18 (*3*). The enzyme consists of three domains: an all-β-strand amino terminal domain similar to fibronectin type III domain, a catalytic β/α TIM-barrel and a small $\alpha+\beta$-fold domain (*7*). It was proposed that a long groove, located at the carboxy-terminal end of the β-strands of the barrel, binds the substrate (*3*, *8*). Multiple alignment of family 18 of glycosyl hydrolases shows conservation of [DN]-G-[LIVMF]-[DN]-[LIVMF]-[DN]-x-E motif (residues 308−315 in *S. marcescens* ChiA) (*9*). The plant seed storage proteins, concanavalin B and narbonin, are members of family 18 known to be devoid of catalytic activity (*10*, *11*). In concanavalin B, a Gln residue replaces the conserved (E) of the above motif and, in narbonin a His residue is found in place of the [DN] in the [DN]-x-E segment (*12*). Very little is known about the mechanism of

* Corresponding author: tel: +30-81-394353 fax: +30-81-394408, e-mail: petratos@imbb.forth.gr. Other author contact information (phone): Y. Papanikolau, G. Tavlas: +30-81-394352, G. Prag: +972-2-6757400, C. E. Vorgias: +30-1-7274514, A. B. Oppenheim: +972-2-6757309.

[§] Foundation for Research and Technology-Hellas.
[||] The Hebrew University.
[⊥] National and Kapodistrian University of Athens.

[1] NAG, 2-*N*-acetyl-D-glucosamine; pNp-diNAG, *p*-nitrophenyl-β-D-N, N′-diacetylchitobiose.

Table 1: Kinetic Parameters of Wild-Type and Mutants of Chitinase A

protein type	K_{cat} (s^{-1})[a]	K_M (μM)[a]	relative K_{cat}/K_M
wild type	331 ± 6.20	52 ± 2	1.0000
D313A	1.6 ± 0.09	296 ± 5	0.0008
E315Q	4.9 ± 0.12	530 ± 9	0.0014
Y390F	1.4 ± 0.10	87 ± 2	0.0025
D391A	1.2 ± 0.11	260 ± 8	0.0007

[a] Kinetic assays were preformed with pNp-diNAG as described in Materials and Methods. Results are average of three independent experiments.

Table 2: Diffraction Data Processing and Refinement Statistics

crystal	E315Q+ (NAG)$_8$	D313A+ (NAG)$_8$	Y390F+ (NAG)$_6$
X-ray source[a]	BW7B	BW7B	BW7A
wavelength (Å)	0.8469	0.8469	1.0000
resolution limit (Å)	10.0−1.9	10.0−1.8	10.0−1.8
data redundancy[b]	4.1 (4.1)	3.7 (3.4)	3.6 (2.9)
completeness (%)[b]	99.0 (100.0)	97.7 (99.0)	93.7 (96.8)
$\langle I/\sigma(I)\rangle$[b]	16.5 (5.9)	24.4 (7.7)	23.4 (6.2)
R_{merge} (%)[b]	5.0 (24.2)	3.4 (14.7)	6.1 (18.0)
R_{factor}/R_{free} (%)[c]	17.3/21.7	17.8/21.7	18.4/22.9
no. of protein atoms	4190	4183	4168
no. of heteroatoms	113	113	99
no. of ordered waters	806	863	773
rms-deviations			
bond length (Å)	0.012	0.012	0.012
bond angle (Å)	0.028	0.026	0.027
mean atomic B values			
protein atoms (Å^2)	22.6	21.8	23.5
substrate (Å^2)	41.4	43.6	40.1

[a] BW7A and BW7B are EMBL/DESY synchrotron beam lines. [b] The numbers in parentheses are statistics from the highest resolution shell as reported by *SCALEPACK*. [c] R_{free} is an R_{factor} calculated with a test set of a random 5% of the diffraction data. $R_{merge} = \Sigma|I_i - \langle I\rangle|/\Sigma\langle I\rangle$; $R_{factor} = \Sigma|F_o - F_c|/\Sigma|F_o|$; I is intensity, F_o, and F_c are observed and calculated structure factor amplitudes, respectively.

action of ChiA partly due to the absence of any oligo-NAG/ChiA complex structure. It was proposed that Glu315 and Asp391 participate in an acid−base catalysis (*7*). In contrast, catalysis was recently proposed to take place via a "substrate assisted" mechanism in which the acetamido O7 of the −1 NAG acts as a nucleophile (*8, 13−16*).

To elucidate the catalytic mechanism of ChiA, we carried out high-resolution crystallographic analysis of the native enzyme. We introduced a number of single point mutations that allowed us to obtain cocrystals with the short forms of substrate. The structures of the complexes of the ChiA mutants E315Q and D313A with octa-*N*-acetyl-chitooctaose (NAG)$_8$ and those of D391A and Y390F with hexa-*N*-acetyl-chitohexaose (NAG)$_6$ provided new insight into the enzymatic mechanism of ChiA.

EXPERIMENTAL PROCEDURES

Site-Directed Mutagenesis. Site-specific mutations were introduced by PCR. The full-length PCR products of wild type and mutated genes were digested by *EcoR*I and *Hind*III restriction endonucleases and cloned into these sites of the pKK223-3 plasmid to give pGPchiA wild-type and mutant clones. Transformation of the ligated DNA was performed by electroporation into *E. coli* XL2B competent cells. Mutant clones were grown on LB plates supplemented with 50 μg/mL ampicillin, colloidal chitin, IPTG (isopropyl-β-D-thiogalactopyranoside) and 5-bromo-4-chloro-3-indolyl-*N*-acetyl-β-D-glucosamine (X-NAG) at 37 °C. Mutant colonies were recognized by their inability to degrade chitin and by the slow conversion of X-NAG. Candidate clones were grown overnight in LB containing 50 μg/mL ampicillin and assayed for chitinase expression by using the substrate pNp-diNAG and by running crude protein extracts of each clone on SDS−PAGE. Wild type and mutant clones were confirmed by DNA sequencing.

Determination of Kinetic Parameters. Enzymatic activity was assayed by the increase in optical density of 405 nm, at 42 °C in reaction mixtures containing a constant concentration of pure enzyme in 100 mM phosphate buffer pH 6.8 and increasing concentration of pNp-diNAG from 1.0 μM to 2.5 mM. The initial rate of hydrolysis was determined for each assay and K_M and K_{cat} were calculated from an average of three experiments by the Michaelis−Menten equation using Prism 2.0 software (GraphsPad). The data are shown in Table 1.

Enzyme Purification and Crystallization. We have improved the overproduction and purification protocol of the enzyme (manuscript submitted). This protocol has been followed for the mutants. The mutant proteins were not secreted to the growth medium, and they had to be extracted from the periplasmic fraction of the bacterial cell-paste. Crystals of the mutants were produced in hanging drops, over a period of 3−4 days at 18 °C. Drops of 6 μL containing 4 μL of 0.5 mM (30 mg mL^{-1}) protein and 2 μL of reservoir solution were equilibrated against 1 mL of reservoir solution consisting of 0.75 M sodium citrate (pH 7.2) and 20% (v/v) methanol. In the cocrystallization experiments, the substrates (Sigma-Aldrich, Ltd.) were added to the drop to a final concentration of 5 mM. All the crystallization experiments were carried out under the same conditions and time scale.

Data Collection, Processing, and Structure Refinement. The crystals were frozen by immersion into liquid N$_2$, and data collections were carried out at 100 °K. All crystals studied belong to the face-centered orthorhombic space group $C222_1$ and exhibited only minor variations in their unit cell dimensions. All data collected were integrated and scaled with the programs *DENZO/SCALEPACK* (*17*).

The refined structure of native ChiA at 1.55 Å resolution, served as the starting point for the restrained refinement of the complexes. The *CCP4* suite (*18*) of programs was employed. The final models were built using *O* (*19*) and *ARP* (*20*) and refined with *REFMAC* (*21*). Finally, the structures were checked for integrity by *PROCHECK* (*22*). The summary of the data collection, processing, and refinement results is shown in Table 2. The figures were produced with *BOBSCRIPT* (*23*) and *GRASP* (*24*) programs.

RESULTS

Construction of Chitinase A Mutant Proteins. To obtain ChiA/oligo-NAG cocrystals, we constructed a number of mutants that are defective in catalysis, by site-directed mutagenesis. To test the importance of specific residues for enzymatic activity, we determined the kinetic parameters of the purified wild-type and mutant proteins. The mutations D313A and E315Q caused about a 100-fold reduction in K_{cat}. Mutations Y390F and D391A were similarly inactive. Qualitatively similar results were obtained with the substrate
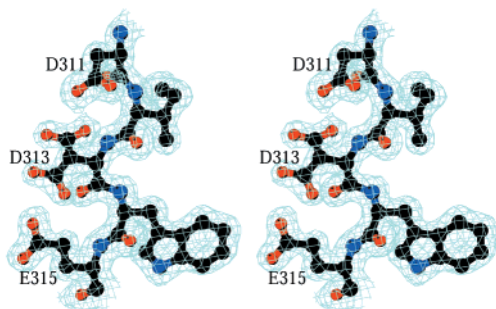
FIGURE 1: Refined structure of native chitinase A. Stereoview of residues Asp311 to Glu315. The side chain of residue Asp313 clearly adopts two conformations of equal occupancy. The electron density map shown is weighted $2F_o - F_c$ contoured at 1σ level. Defocused representation of the stereoimages is used in all figures.

4-methyl-umbelliferyl-diNAG. We further note that the mutations D313A, E315Q, and D391A increase K_M. We also generated the mutations D391E and D391N that resulted in only a minor reduction of ChiA activity (data not shown).

Characterization of the Catalytic Site. The native ChiA structure refined at 1.55 Å (manuscript submitted) revealed among others the following striking feature. The side chain of residue Asp313, which lies in the active site, adopts two conformations as shown in Figure 1. In one conformation, it interacts with the catalytic, proton donor residue Glu315. In the other conformation, it interacts with the conserved Asp311. The mutants E315Q and D313A enabled us to obtain cocrystals with the intact $(NAG)_8$. The refined structures of the complexes $E315Q+(NAG)_8$ and $D313A+(NAG)_8$ are essentially the same. In addition, the structures of the mutants show no significant changes as compared to the native refined enzyme. The overall structure of the complex $E315Q+(NAG)_8$ is shown in Figure 2a,b. The substrate can be clearly seen firmly embedded within the deep semi-closed tunnel (about 8−11 Å in width and about 15 Å deep) of the enzyme. The structures of the complexes show that a large number of amino acid residues contribute to the binding of $(NAG)_8$. Table 3 presents the interactions between E315Q and the bound chito-oligosac-charide. The enzyme recognizes at least the sugar residues at subsites +2, +1, and −1 (*25*). The most significant of the enzyme−substrate contacts are localized in this area. Aromatic and charged residues mediate the contacts. Weaker interactions extend from −2 to −6 subsites. Finally, a number of interactions of −5 and −6 sugar residues are due to the packing in the crystal lattice and do not reflect any biological function. Close-up views of the subsites +2, +1, and −1 for the complexes $E315Q+(NAG)_8$ and $D313A+(NAG)_8$ are shown in Figure 3a and b, respectively. The oligosaccharide bound to the active site is rotated and bent at the cleavage region, i.e., at the sugar units at subsites −1 and +1. Substrate distortion in glycosyl hydrolysis was also previously suggested (*26, 27*). We find that the sugar residue bound at subsite −1 adopts a "boat" $^{1,4}B$ conformation unlike the 4-sofa conformation reported for the structure of chitobiase$+(NAG)_2$ complex (*28*) and the modeled structure of the ChiA complex with $(NAG)_6$ (*8*). In the complexes of D313A and E315Q, all the acetamido groups are pointing away from their corresponding sugar rings and assume an energetically favorable conformation. In particular, the acetamido group of sugar residue at subsite −1, in the
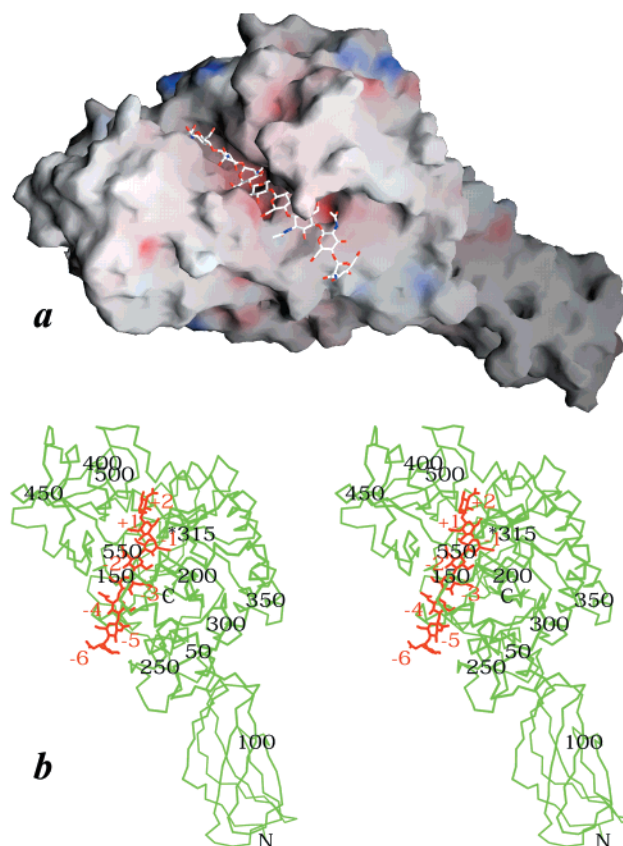

FIGURE 2: Substrate complex with inactive chitinase A mutant E315Q. (a) Octa-*N*-acetyl-chitooctaose $(NAG)_8$ bound to the long semiclosed tunnel of the enzyme. The substrate is rotated and bent in the vicinity of the scissile bond (subsites −1, +1). Sugar residue at −1 assumes a "boat" conformation. (b) Stereoview of the uncleaved $(NAG)_8$ (shown in red) on the enzyme's Cα tracing (shown in green).

Table 3: Interactions between Chitinase A Mutant E315Q and Bound Substrate $(NAG)_8$

protein residues	subsites for sugar residues[a]
W275, K369, D391, F396, Y418	+2
W275, Q315, F316, M388, D391, R446[b]	+1
Y163, W275, D313, Q315, A362, M388, Y390[b], D391, Y444, R446, W539	−1
W275, T276, E473, W539, E540	−2
W167, T276, E473	−3
R172	−4
N70[c], Y170	−5
Y170, F232, K237[b]	−6

[a] Nomenclature for sugar subsites as in ref *25*. Residue at +2 is the reducing end of the oligosaccharide. Interactions involve at least one atom of each amino acid residue at a distance ≤ 3.6 Å from an atom of the corresponding sugar ring. [b] The interactions are mediated also by water molecules. [c] N70 belongs to a symmetry related $(x, 1−y, −z)$ ChiA molecule in the crystal lattice.

complexes of D313A and E315Q is pointing toward residues 313 and 315 (Figure 3a,b). In the structure of $E315Q+(NAG)_8$ the acetamido group of −1 sugar can also assume a second conformation with 30% occupancy that directs toward Tyr390. In this conformation atom O7 (carbonyl oxygen) replaces the water molecule that is H-bonded to the phenol hydroxyl of Tyr390. The latter conformation of −1 acetamido group is not shown in Figure 3a for the sake of clarity. To allow for the major, energeti-
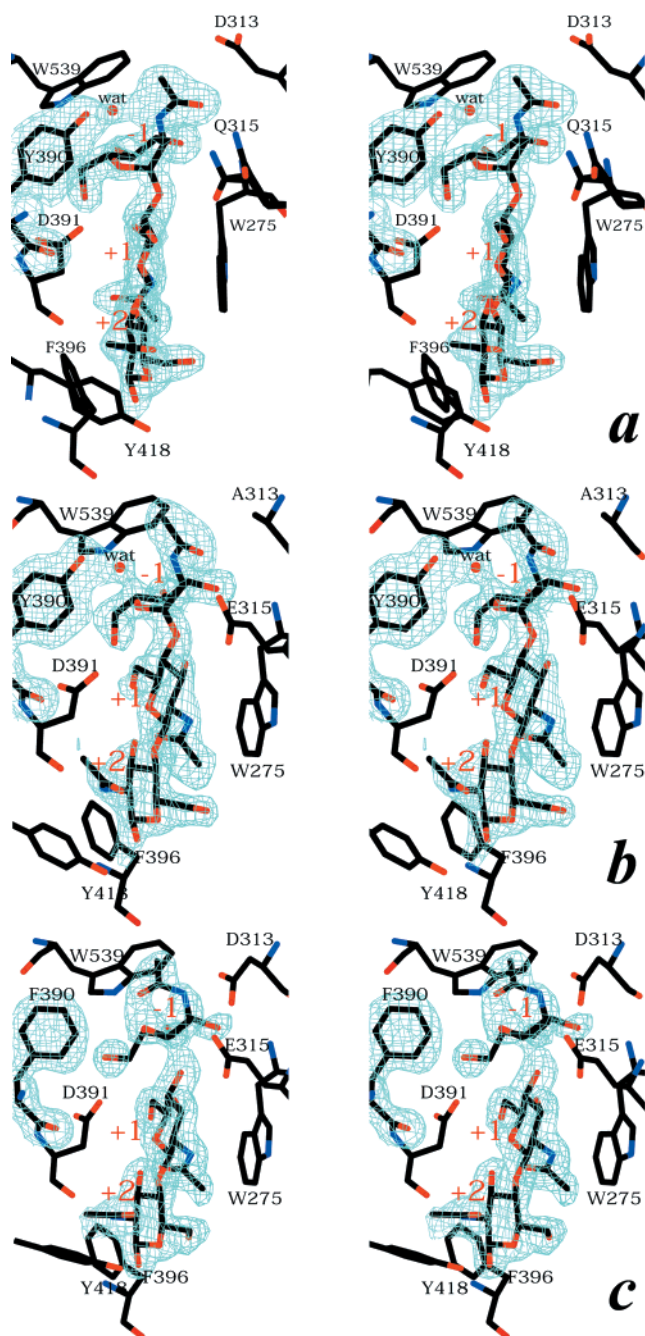
FIGURE 3: Active site region of chitinase A mutants. (a) Stereoview of the oligosaccharide bound at subsites +2, +1, and −1 of the E315Q mutant. Gln315 assumes two conformations. The second possible conformation for −1 acetamido toward Tyr390 is not shown for the sake of clarity. (b) Stereoview of the oligosaccharide bound at subsites +2, +1, and −1 of the D313A. In panels a and b, the 2-acetamido group of −1 sugar points away from the pyranose ring. In both structures, one water molecule (wat) is H-bonded to both phenyl hydroxyl of Tyr390 and NH of 2-acetamido group of −1 sugar residue. (c) Stereoview of the oligosaccharide bound at subsites +2, +1, and −1 of the Y390F mutant. In this complex, there is no water bound to the NH group of −1 sugar residue. In this structure, the glycosidic bond between −1 and +1 sugar residues is cleaved, but hydrolysis is not completed. In all mutants, the −1 sugar residue adopts a "boat" $^{1,4}B$ conformation. The aromatic residues Phe396, Trp275, and Trp539 recognize mainly the +2, +1, and −1 sugar residues, respectively. Residue Asp391 interacts with all three sugar units. Tyr418 is proposed to be the "docking" residue for the reducing end of the oligosaccharide. The electron density maps shown are weighted $2F_o − F_c$ contoured at 1σ level.

cally favorable conformation of −1 acetamido group, Asp313 is directed toward Asp311. In D313A, the absence of the side chain leads to a similar result. Gln315 (Figure 3a) assumes two conformations. The flexibility of this residue in the mutant protein may have no relevance to the catalytic activity. In the complex D313A+(NAG)$_8$, we also observe a water molecule H-bonded to phenol hydroxyl of Tyr390 and the ring oxygen O5 of sugar residue at subsite −1 (Figure 3b). In our structures, the reducing-end sugar residue at subsite +2 marks the end of the bound substrate. Moreover, while the chito-oligosaccharides used for the cocrystallizations are in equilibrium between the α and β configurations of the reducing-end anomeric carbon, only the β stereoisomer is observed in the analyzed structures.

The Importance of Tyrosine 390. We aligned the structures of the ChiA complex with allosamidin (manuscript submitted) and the corresponding hevamine complex (13, 29) based on the allosamidin coordinates. Moreover, we aligned the structures of the complexes E315Q+(NAG)$_8$ and chitobiase+(NAG)$_2$ (28) based on the coordinates of the −1 and +1 sugar residues. The structural alignments revealed the conservation of one tyrosine residue in all three enzymes. The conserved tyrosine was also identified in the known structures of endo-β-N-acetylglucosaminidases F$_1$ (30) and H (31). Sequence alignment of family 18 chitinases shows that this tyrosine residue (Tyr390 in ChiA) is highly conserved. We find that Tyr390 binds one water molecule observed in the structures E315Q+(NAG)$_8$ and D313A+(NAG)$_8$. To investigate the role of Tyr390 and the significance of the water molecule bound to it, we designed the mutant Y390F. The structure of the latter mutant cocrystallized with (NAG)$_6$ provided additional information for the catalyzed reaction. In the electron density map, we identified a partially cleaved glycosidic bond between sugar residues −1 and +1. The distance between C1(−1) and O4(+1) is 1.97 Å (C−O bond length is 1.39 Å, estimated standard error for bond lengths is 0.19 Å). In the complex of this mutant, the water molecule is absent and a disaccharide is clearly bound at subsites +1 and +2 (Figure 3c) with an average value of atomic temperature factor (B) 32.3 Å^2. We also located, though with higher thermal parameters (43.3 Å^2), the remaining of the substrate bound at subsites −1 to −5. The additional observed sugar residue modeled at −5 subsite is due to the presence of a certain amount of (NAG)$_7$ in the purchased (NAG)$_6$. In this structure, carbonyl oxygen O7 of the −1 acetamido group lies 1.8 Å from atom O5 and 2.6 Å from anomeric carbon C1 of the −1 pyranose ring. The distance to the anomeric carbon C1 does not support potential formation of an oxazoline intermediate as it was initially proposed (8). Moreover, atom O7 comes close to the −1 sugar ring because of the lack of phenol hydroxyl in the mutant Y390F.

To investigate the role of Asp391, we cocrystallized D391A with (NAG)$_6$. The analysis of the structure of the complex reveals that the substrate is actually cleaved during the cocrystallization step (data not shown). The disaccharide product of ChiA exhibits preferential binding at sites +1 and +2. The same was observed earlier (8) in the complex of native ChiA crystals soaked with (NAG)$_4$.

DISCUSSION

The structures of the complexes E315Q and D313A with substrate reveal only one ordered water molecule in the active site that is H-bonded to the phenol hydroxyl of Tyr390 and the NH group of the 2-*N*-acetyl of the −1 sugar moiety. As the access of water molecules from the bulk solvent area to the occupied catalytic site is stereochemically hindered, we conclude that this water molecule is there because it participates in the reaction. The observed double conformation of Asp313 of the refined native ChiA structure in conjunction with the two distinct orientations observed for the 2-*N*-acetyl group of the −1 sugar, provide the following proposed mechanism for one cycle of hydrolysis by chitinase A.

Binding of Substrate, Protonation and Cleavage of the Glycosidic Bond. According to our crystallographic data, we propose that in the substrate free enzyme Glu315 is protonated due to its proximity to Asp313. In the enzyme−substrate complex, the acetamido group of the −1 sugar lies away from the aldohexose ring, as can be seen in the case of D313A and E315Q complexes (Scheme 1a) and assumes an energetically favorable conformation. To allow for the latter conformation of the acetamido group, the side chain of Asp313 points toward Asp311. Upon binding, the enzyme imposes to the −1 sugar the following conformational change. The stable "chair" conformation $^4C_1$ becomes "boat" $^{1,4}B$, thus raising the free energy of the substrate by approximately 8 kcal/mol (*32*). This conformational change participates in the bending and rotating of the bound oligosaccharide. At this stage, one water molecule is H-bonded to both the phenol hydroxyl of Tyr390 and the NH of the acetamido group of the −1 sugar.

Subsequently, the protonated γ-carboxylic group of Glu315 donates its proton to oxygen O4 of +1 sugar residue, thus cleaving the glycosidic C1(−1)-O4(+1) bond. The protonation and reversible cleavage of the glycosidic linkage induces the following: (i) rotation of Asp313 side-chain toward Glu315 and (ii) rotation of the −1 acetamido group around its C2−N2 bond toward Tyr390. The rotation of the acetamido group results in translocation of the water molecule that was originally bound to Tyr390, to the opposite side of the sugar ring and close to Glu315 (Scheme 1b). The chemical entities that stabilize the positive charge developed on atoms C1 and O5 of −1 sugar are the deprotonated γ-carboxylate of Glu315, the water that is H-bonded to Tyr390 and −1 acetamido group, the Sδ sulfur of Met388 and the O7 atom of −1 acetamido group. Following the cleavage, the sugar residue at subsite −1 shifts away from the residue at subsite +1. At this stage, the water molecule is poised to the anomeric C1 carbon of −1 sugar from the same side as the departed oxygen O4 of the +1 sugar. The close proximity of Asp313 and Glu315 forces the following: (a) uptake of a proton from the water by the γ-carboxylate of Glu315 and (b) uptake of the remaining hydroxide anion by the C1 carbon of −1 sugar. This step completes a hydrolytic cycle of the enzyme.

Products of Hydrolysis. In the case of tri- or tetrasaccharides, the sugar residues at subsites −1 and −2 are released from the active site (Scheme 1c). This is observed in the structure of native ChiA complex with (NAG)$_4$ (*8*). In the case of a pentasaccharide, the trisaccharide moiety bound at

Scheme 1: Proposed Mechanism of Catalysis by Chitinase A[a]
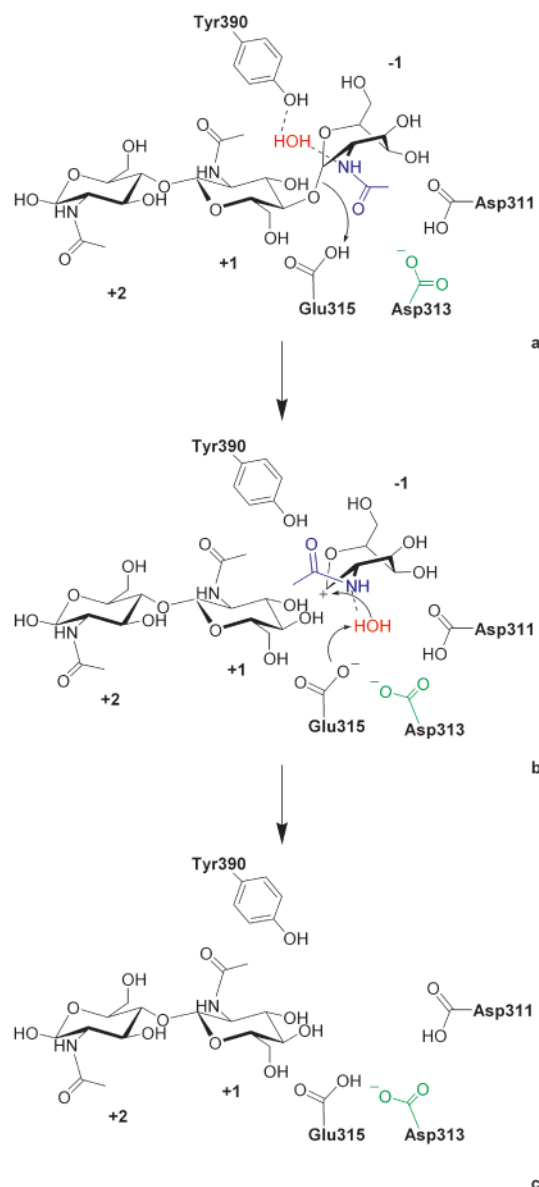
[a] (a) A trisaccharide is shown bound to subsites +2, +1, and −1. The −1 sugar unit assumes a "boat" conformation, and the 2-*N*-acetyl group (shown in blue) is pointing toward residues Asp313 (shown in green) and Glu315. Glu315 is protonated and poised to cleave the glycosidic linkage between −1 and +1 sugar residues. One water molecule (shown in red) is H-bonded to the phenol hydroxyl of Tyr390 and to the NH of the 2-*N*-acetyl group. The proposed "Michaelis complex" is based on the combination of the solved structures of E315Q+(NAG)$_8$ and D313A+(NAG)$_8$. (b) The approach of acidic residue Asp313 toward Glu315 forces the acetamido group of −1 sugar to rotate around its C2−N2 bond, thus displacing the water molecule into the vicinity of Glu315. The partially cleaved intermediate of the trisaccharide is shown. A proton from the water molecule will be taken up by the γ-COO$^-$ of Glu315 and the remaining hydroxide ion will be taken up by the anomeric C1 atom of −1 sugar residue. The proposed reaction intermediate is based on the solved structure of Y390F+(NAG)$_6$. (c) Hydrolysis is completed. The monosaccharide departs from subsite −1, and the disaccharide remains bound at the enzyme subsites +1, +2. The proposed enzyme−product complex is based on the solved structures of D391A+(NAG)$_6$ and native ChiA crystals soaked with (NAG)$_4$ (*8*).

subsites −1, −2, and −3 slides forward in the active site and releases the di-saccharide bound at subsites +1 and +2. In the case of longer substrates, catalysis occurs until the

"minimal" substrate (tri- or tetrasaccharide) is hydrolyzed. This is observed in the structure of D391A+(NAG)$_6$. ChiA is known to act via a retaining mechanism (*33*). This implies that the β configuration of the anomeric carbon is retained after hydrolysis. Our refined structures show that only the β stereoisomer is observed from a mixture of both α and β isomers at the reducing end of the sugars. These results in combination with the observed semiclosed tunnel shape of the active site (Figure 2a) strongly suggest a processive character of hydrolysis by ChiA. The proposed mechanism is in accordance with the potent ChiA inhibition ($K_i = 100$ nM) by allosamidin (*34*). The natural inhibitor binds strongly to the enzyme subsites -1 to -3 (manuscript submitted) thus preventing the entrance of substrate into the proper place of the active site for hydrolysis to occur.

The earlier proposed catalytic mechanism that invoked substrate assistance (*8*) imposes that the carbonyl oxygen of the -1 acetamido moiety has to form a covalent bond to the corresponding anomeric carbon C1. We cannot observe an oxazoline ring intermediate. In the structure of Y390F+(NAG)$_6$ that simulates an intermediate of the reaction, the acetamido group of -1 sugar comes close to O5 atom in a way that could allow a modified "substrate assisted" reaction, although there are several chemical entities as mentioned above that can serve as nucleophile of this general acid–base catalysis. Moreover, according to the earlier mechanism the protonated $+1$ sugar residue is proposed to leave the active site. This is observed in the case of hevamine where only subsites -1 to -4 are occupied by (NAG)$_4$. In ChiA, the protonated $+1$ sugar residue leaves the active site last. This is observed in all ChiA complexes.

On the basis of the above-described structures, ChiA could be mainly an exo-chitinase and in particular, a chitobiosidase that cleaves (NAG)$_2$ units from the reducing end of chitin. These findings fit with the recent structural observation that chitinase B from *S. marcescens* is a chitotriosidase (*35*) that cleaves chitotriose units from the nonreducing end of chitin. The two enzymes along with chitobiase and chitinase C (*36*), from the same organism may act synergistically to degrade chitin more efficiently.

ACKNOWLEDGMENT

REFERENCES

1. *Chitin Handbook* (1997) Muzzarelli, R. A. A., Peter, M. G. Eds., European Chitin Society, Grottammare, Italy.
2. Sahai, A. S., and Manocha, M. S. (1993) *FEMS Microbiol Rev. 11*, 317−338.
3. Henrissat, B., and Bairoch, A. (1996) *Biochem. J. 316*, 695−696.
4. Boot, R. G., Renkema, G. H., Strijland, A., van Zonneveld, A. J., and Aerts, J. M. (1995) *J. Biol. Chem. 270*, 26252−26256.
5. Saito, A., Ozaki, K., Fujiwara, T., Nakamura, Y., and Tanigami, A. (1999) *Gene 239*, 325−331.
6. Boot, R. G., Blommaart, E. F., Swart, E., Ghauharali-van der Vlugt, K., Bijl, N., Moe, C., Place, A., and Aerts, J. M. (2001) *J. Biol. Chem. 276*, 6770−6778.
7. Perrakis, A., Tews, I., Dauter, Z., Oppenheim, A. B., Chet, I., Wilson, K. S., and Vorgias, C. E. (1994) *Structure 2*, 1169−1180.
8. Tews, I., Terwisscha van Scheltinga, A. C., Perrakis, A., Wilson, K. S., and Dijkstra, B. W. (1997) *J. Am. Chem. Soc. 119*, 7954−7959.
9. Hofmann, K., Bucher, P., Falquet, L., and Bairoch, A. (1999) *Nucleic Acids Res. 27*, 215−219.
10. Hennig, M., Pfeffer-Hennig, S., Dauter, Z., Wilson, K. S., Schlesier, B., and Nong, V.-H. (1995) *Acta Crystallogr. Sect. D 51*, 177−189.
11. Hennig, M., Jansonius, J. N., Terwisscha van Scheltinga, A. C., Dijkstra, B. W., and Schlesier, B. (1995) *J. Mol. Biol. 254*, 237−246.
12. Terwisscha van Scheltinga, A. C., Hennig, M., and Dijkstra, B. W. (1996) *J. Mol. Biol. 262*, 243−257.
13. Terwisscha van Scheltinga, A. C., Kalk, K. H., Beintema, J. J., and Dijkstra, B. W. (1994) *Structure 2*, 1181−1189.
14. Knapp, S., Vocadlo, D., Gao, Z., Krik, B., Lou, J., and Withers, S. G. (1996) *J. Am. Chem. Soc. 118*, 6804−6805.
15. Kobayashi, S., Kiyosada, T., and Shoda, S.-I. (1996) *J. Am. Chem. Soc. 118*, 13113−13114.
16. Brameld, K. A., Shrader, W. D., Imperiali, B., and Goddard III, W. A. (1998) *J. Mol. Biol. 280*, 913−923.
17. Otwinowski, Z., and Minor, W. (1997) *Methods Enzymol. 276*, 307−326.
18. Bailey, S. (1994) *Acta Crystallogr. Sect. D 50*, 760−763.
19. Jones, T. A., Zou, J. Y., Cowan, S. W., and Kjeldgaard, M. (1991) *Acta Crystallogr. Sect. A 47*, 110−119.
20. Lamzin, V. S., and Wilson, K. S. (1997) *Methods Enzymol. 277*, 269−305.
21. Murshudov, G. N., Vagin, A. A., and Dodson, E. J. (1997) *Acta Crystallogr. Sect. D 53*, 240−255.
22. Laskowski, R. A., MacArthur, M. W., Moss, D. S., and Thornton, J. M. (1993) *J. Appl. Crystallogr. 26*, 283−291.
23. Esnouf, R. M. (1997) *J. Mol. Graph. Model. 15*, 132−134.
24. Nicholls, A., Sharp, K. A., and Honig, B. (1991) *Proteins 11*, 281−296.
25. Davies, G. J., Wilson, K. S., and Henrissat, B. (1997) *Biochem. J. 321*, 557−559.
26. Blake, C. C., Johnson, L. N., Mair, G. A., North, A. C., Phillips, D. C., and Sarma, V. R. (1967) *Proc. R. Soc. London B Biol. Sci. 167*, 378−388.
27. Phillips, D. C. (1966) *Sci. Am. 215*, 78−90.
28. Tews, I., Perrakis, A., Oppenheim, A., Dauter, Z., Wilson, K. S., and Vorgias, C. E. (1996) *Nat. Struct. Biol. 3*, 638−648.
29. Terwisscha van Scheltinga, A. C., Armand, S., Kalk, K. H., Isogai, A., Henrissat, B., and Dijkstra, B. W. (1995) *Biochemistry 34*, 15619−15623.
30. van Roey, P., Rao, V., Plummer, T. H., Jr., and Tarentino, A. L. (1994) *Biochemistry 33*, 13989−13996.
31. Rao, V., Guan, C., and Van Roey, P. (1995) *Structure 3*, 449−457.
32. Dowd, M. K., French, A. D., and Reilly, P. J. (1994) *Carbohydr. Res. 264*, 1−19.
33. Davies, G., and Henrissat, B. (1995) *Structure 3*, 853−859.
34. Spindler, K.-D., and Spindler-Barth, M. (1999) *EXS 87*, 201−209.
35. van Aalten, D. M. F., Synstad, B., Brurberg, M. B., Hough, E., Riise, B. W., Eijsink, V. G. H., and Wierenga, R. K. (2000) *Proc. Natl. Acad. Sci. U.S.A. 97*, 5842−5847.
36. Suzuki, K., Taiyoji, M., Sugawara, N., Nikaidou, N., Henrissat, B., and Watanabe, T. (1999) *Biochem. J. 343*, 587−596.